4
Effect of Surface Morphology on the Memory Devices Based on Polymer-Small Molecule Blend

The surface morphology of the active layer plays an important role in the switching mechanism of organic molecular memory devices. Small pinholes in the morphology of the active layer are supportive of the metallic filament formation whereas the big pits in the active layer provide the direct pathway between the electrodes and hence no switching is observed. In the present study, the surface morphology is controlled with the rotational speed of the spin coating process. At lower speeds of rotation, the solution which is spin coated on the substrate is allowed to settle, hence the phase segregation occurs during the process which causes the formation of large pits and valleys. At the higher speed, the time allowed for phase segregation is less, hence the smaller pinholes are formed on the surface of the active layer. In the present study, we have tuned the ON-OFF ratio of the polymer-small molecule blend memories [Vyas *et al.*, 2018].

4.1 INTRODUCTION

Conventional electronics have been dependent on the silicon-based devices heavily. The silicon-based memories are practically everywhere in this era of information technology. The current processors have billions of transistors on a single chip, still, the demand for higher performance is ever increasing. The performance increases with the number of transistors per unit area which is now approaching towards a saturation level. Any significant increase in the performance now can be achieved by a paradigm shift in the technology used. Organic molecular memories may prove themselves as a milestone in removing this bottleneck. Unlike silicon-based memories, the organic memories are dependent on the resistive switching which shows two different levels of conductance at the same voltage level.

As discussed earlier there are many switching mechanisms available for the organic molecular memories e.g. electrochemical redox of the material [Li *et al.*, 2004], ferroelectricity [Furukawa, 1989], resistive switching of MIM memories [Kiguchi and Fujii, 2017], charge transfer complex (CTC) [Zhengchun *et al.*, 2006], and presence of floating metallic islands [Ma *et al.*, 2002; Ma *et al.*, 2002]. Filament formation is another mechanism of switching which has been in focus recently in the field of organic molecular memories [Cölle *et al.*, 2006].

Here in this study, the exponential increase in the ON-OFF ratio has been shown in the polymer-small molecule blend devices. In this study, the aspect of filament formation has been explored further with the tuning of the surface morphology of the active layer. The surface morphology of the active layer is controlled with the change in the rpm of rotation of the substrate while spin coating. The switching mechanism is validated with the observation of the surface morphology of the film used for device fabrication. The surface contains either larger valleys or smaller pinholes. The devices with larger pits and valleys show a poor switching characteristic whereas the devices with smaller pinholes show a large ON-OFF ratio and superior switching characteristics.

4.2 EXPERIMENTAL SECTION

Indium tin oxide (ITO) coated glass substrates were used for the fabrication of the devices. The substrates were procured from Techinstro, India. To make a crossbar architecture, the bottom ITO layer was etched into a strip with the help of HCl and zinc dust. The central strip was

protected using tape. To clean the substrates, they were ultrasonicated in soap solution. Cleaning in soap solution was followed by a thorough rinse in de-ionized (DI) water. The substrates were further ultrasonicated in acetone, DI water, and methanol thrice in each solution. For each repetition of ultrasonication, the fresh solvent was used. The substrates were then dried in a vacuum oven for a few hours at 70 °C.

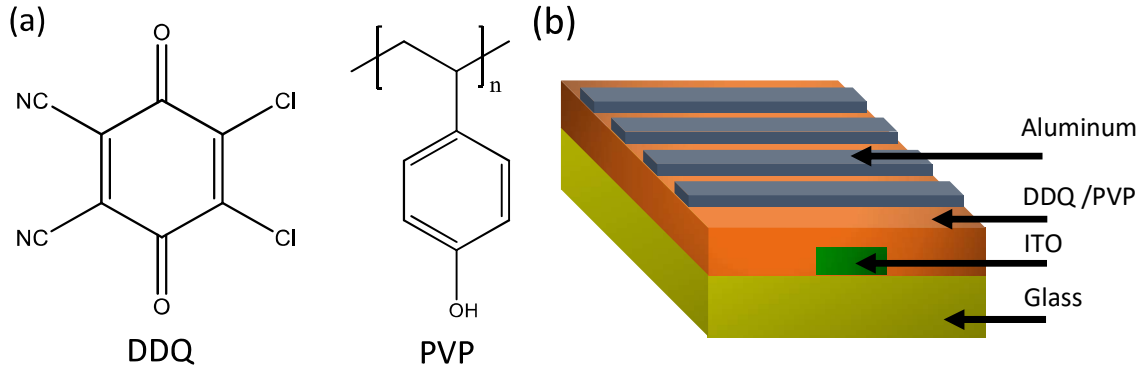

Figure 4.1: (a) Molecular structures of DDQ and PVP (b) schematic of the ITO/PVP:DDQ/Al device structure; the crossbar architecture makes sure that the probes don't short circuit the device while IV characterization.

The active layer was deposited on the substrates using the spin-coating process. 2,3-Dichloro-5, 6-dicyano-1,4-benzoquinone (DDQ) and poly(4-vinyl phenol) (PVP) are the active materials which were used for the deposition on the substrate. All chemicals were procured from Aldrich Co. and were used without any further purification. Figure 4.1(a) shows their molecular structures. Solutions were prepared in isopropyl alcohol (IPA), with a concentration of 25 mg/ml. The weight ratio for DDQ and PVP was chosen to be 60:40. The active layers were deposited at rotational speeds varying from 1000 to 5000 rpm with an increment of 1000rpm. Films were kept for drying in room temperature for 6-7 h. After drying, the top aluminum electrodes were deposited with the thermal deposition method in high vacuum. For making a crossbar architecture, the shadow mask was kept on top of the active layer with striped windows being perpendicular to the bottom ITO strip. The area of each memory cell thus prepared is around 0.25 mm^2. The thickness of Al deposited on top is 50 nm. The schematic of the structure of ITO/DDQ:PVP/Al based MIM devices thus prepared is shown in figure 4.1(b).

Thickness measurements on the active organic layers were carried out using Bruker Dektak XT-100 profilometer. The thickness of the films varied with rotational speeds. For 1000 rpm, an average thickness of 418 was recorded and the standard deviation of 34 nm was observed. For devices with 5000 rpm, an average thickness of 106 nm was observed with a standard deviation of 11 nm. The UV-visible absorption spectra for thin films as well as the solution was measured using Shimadzu UV1800 UV-visible spectrophotometer. For measurement of the absorbance spectra of thin-films in the UV range, the films were deposited on the quartz substrates under the same conditions as those of the devices under study. The topography of the active layers was investigated using Park Systems XE-70 atomic force microscope (AFM). AFM measurements were carried out in the non-contact mode with a soft tapping tip. The scan rate for the measurements was 0.4 lines per second. A total of 256-512 lines were scanned in a frame, with the number of pixels in one line being same as the number of lines. The scanning electron microscope (SEM) images of cross section of all the devices were taken with a Zeiss EVO18 Scanning Electron Microscope. A homemade vacuum chamber was used for electrical characterization of the devices under a vacuum of the order of 10^{-5} mbar. The IV characterization measurements were taken using a two-probe method with Al being the top electrode and ITO being the bottom contact. The vacuum in the chamber prevents the effect of humidity and oxygen

present in the environment. There is a possibility of probes penetrating the top contact and piercing the active layer all the way to the bottom contact thus creating a short-circuited path between the top and the bottom contacts. This was avoided by the crossbar architecture, because even if the probe penetrates through the active material all the way to the bottom, it makes contact with the glass rather than ITO at the bottom, thus avoiding the problem of a short circuit. The IV characterization was recorded on a remote PC using custom LabView programs, interfaced with the Keithley 6430 subfemtoampere source meter. Many characterizations including voltage sweep, long-run retention test, and repeated write-read-erase-read were carried out on the devices.

4.3 RESULTS AND DISCUSSION

4.3.1 Absorption Spectra

The UV-visible absorbance spectra of the individual materials in solution form in IPA were observed, and for DDQ, the peak was observed at 352 nm, and for PVP, it was observed at 279 nm. The absorbance spectra of the mixture of DDQ and PVP shows the presence of both the materials. The intensity of the peak of the mixture is dominated by DDQ, as can be seen in figure 4.2. The other small hump present in the mixture's spectra is that of the PVP. The absorption spectra of the thin-films had a little shift in the peak positions. This happened due to the difference in the order of crystallinity in the two phases – solid and solution. This also verifies the fact that there are no charge transfer complexes (CTC) formed between the two materials in the mixture either in the solution or in the thin films.

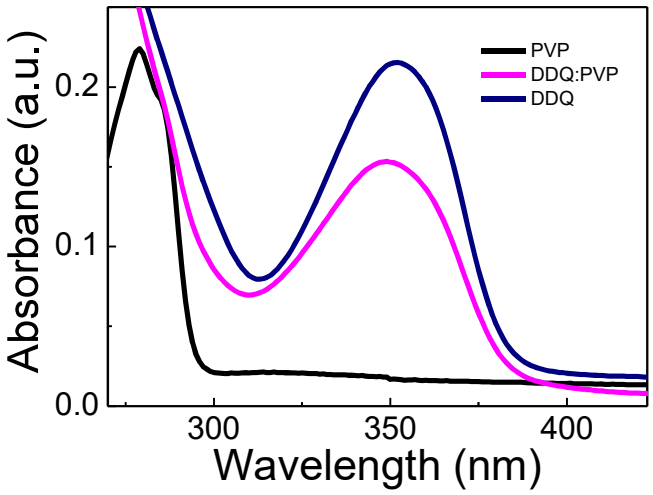

Figure 4.2: The absorbance spectra of individual components along with the mixture of PVP and DDQ.

4.3.2 Surface Morphology Study

It can be clearly seen in figure 4.3 that as the rotational speed at the time of spin coating increases, the surface morphology varies in a distinctive manner. As the concentration of DDQ increases the size of holes varies from very large to small pinholes. For the 1000 rpm devices, the average thickness was found to be 418 nm with a standard deviation of 34 nm. The surface of the samples with 1000 rpm, as shown in figure 4.3(a), are filled with large holes. There are some small island-like structures on the surface. The gap between these structures is more than 1μm. Such large pits make it easy to form a direct conducting path from top to bottom. The AFM image of 2000 rpm devices, as can be seen in figure 4.3(b) show that there are still many islands and small structures on the surface. The thickness of the 2000 rpm device was approximately 245 nm. These structures however, are not separated from each other by a distance as large as in the previous

case. The typical size of the structures is between 400 to 500 nm which is again sufficient to allow a direct path between the top and bottom electrodes after the deposition of Al. As shown in figure 4.3(c), the small and large isolated structures (shown as a green circle and red rectangle respectively) are being continued to form. However, the spacing between those structures is narrow this time. This arrangement makes it possible to allow a narrow pathway between the top and bottom electrode but not necessarily at the time of Al deposition. The formation of a conducting filament requires an application of a suitable voltage bias. The thickness of these films was recorded to be 161 nm. As the rpm increases further, to 4000, the thickness decreases again to a value of 151 nm. It is clear from figure 4.3(d), the surface is fully packed with the small structures of almost similar sizes. In this case, the gap between the small structures is lesser than the previous case. The average thickness for 5000 rpm devices was found to be 106 nm with a standard deviation of 11 nm. As shown in figure 4.3 (e), there are a few pinholes present on the surface. Presence of pinholes allows the formation of a filamentary path between the top and bottom electrodes under suitable voltage bias.

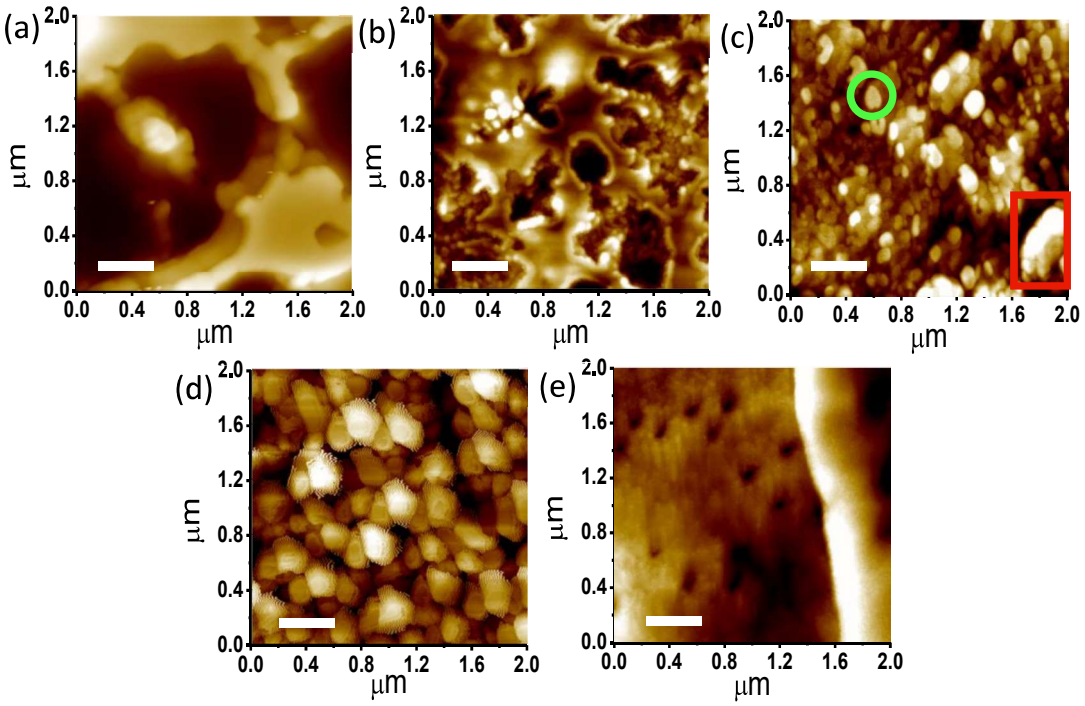

Figure 4.3: (a) – (e) AFM images of the active layers of DDQ and PVP deposited by spin coating at rpms 1000, 2000, 3000, 4000, and 5000. The white bar in each image indicates a distance of 400 nm. The green circle and red rectangle show the small and big structures respectively.

A cross-sectional SEM was also studied for the devices fabricated at different rotational speeds. The cross-sectional scanning electron microscope (SEM) images of devices fabricated at 1000-5000 rpm with an increase of 1000 rpm are shown in figure 4.4 (a)-(e) respectively. The orange, yellow and green colored stripes represent aluminum (Al), the active organic layer, and ITO respectively. The yellow rectangle indicates the portion where the energy dispersive X-ray (EDX) spectra were recorded. The EDX was measured in the active organic layer. Length scales of the images shown in figure 4.4(a) – (e) are 200, 300, 200, 200 nm, and 1μm respectively. The EDX obtained from the areas specified under rectangle tell us the amount of aluminum penetrating the organic layer due to the metallic filament formation via big holes/pinholes present in the surface of the active layer. The contrast shown by the films having larger holes

(such as 1000 rpm devices) is much better even at the lower magnification. On the other hand, the films deposited at higher rpm are smoother because of the presence of smaller pinholes. The normalized elemental percentage of atomic aluminum was found to be 5.62%, 4.2%, 0.97%, 0.9%, and 4.49% for devices prepared at 1000 to 5000 rpm respectively.

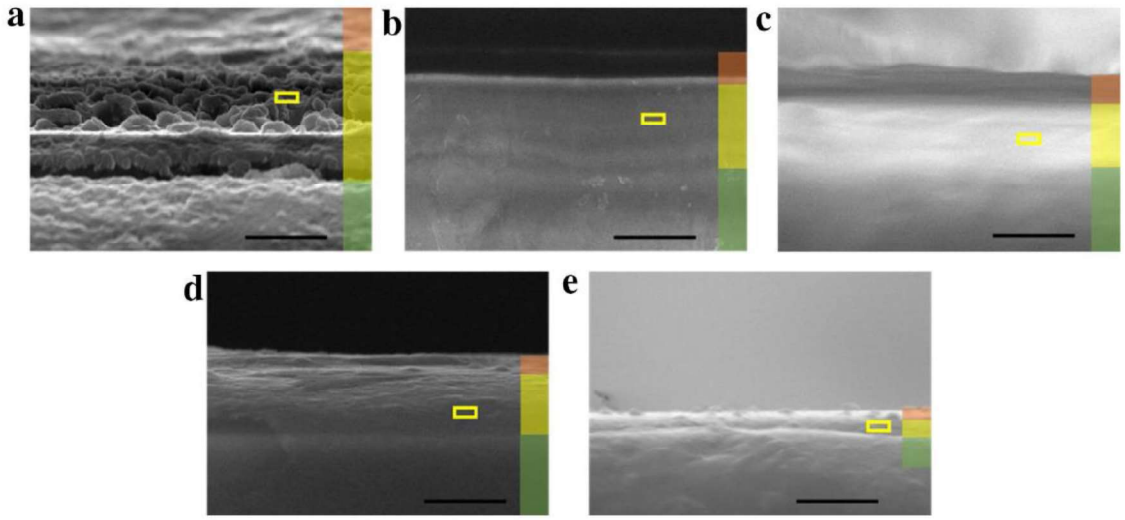

Figure 4.4: (a) – (b) Cross sectional scanning electron microscope (SEM) images of devices deposited at 1000 to 5000 rpm, respectively, with an increment of 1000 rpm. The orange color stripe represents Al, yellow color stripe represents active layer and green color stripe represents ITO in all images. The rectangle represents the spot where the EDX was observed. The horizontal black bar represents distances of 200, 300, 200, 200 nm, and 1μm respectively

4.3.3 Electrical Characterization

The I-V characteristics of the devices with various rpm are shown in figure 4.5. There was a distinct trend in the I-V characteristics with the increasing rpm of rotation. The 1000 rpm-based device showed no switching at all as shown in figure 4.5(a). The current varies almost linearly with the voltage. The absolute value of the current was also high in both negative and positive bias voltage, indicating the presence of a permanent, low resistance path between the top and bottom electrodes. Dashed arrows in figure 4.5(a) show the direction of the voltage sweep. For 2000 rpm devices, although the device shows a semiconducting behavior, there is no switching observed in the I-V curve shown in figure 4.5(b). Hence a very low ON-OFF ratio is observed in the first two devices with 1000 and 2000 rpm. A significant switching is evident in case of the 3000 rpm devices, in the negative bias direction as shown in figure 4.5(c). The highest ON-OFF ratio obtained for this device is 4.8×10^2. Switching continues to occur in the negative bias direction for the 4000 rpm-based device as can be seen in figure 4.5 (d). The highest ON-OFF ratio obtained for this device was 2.4×10^3. The switching continued to appear in the negative bias region for 5000 rpm based devices as shown in figure 4.5(e). The ON-OFF ratio observed in this device was 1.2×10^4. The switching behavior observed in all the devices was consistent with high reproducibility. The maximum ON-OFF ratios for all the devices was plotted against the rpm, and it was found to vary exponentially with respect to the rotational speed as shown in figure 4.5(f).

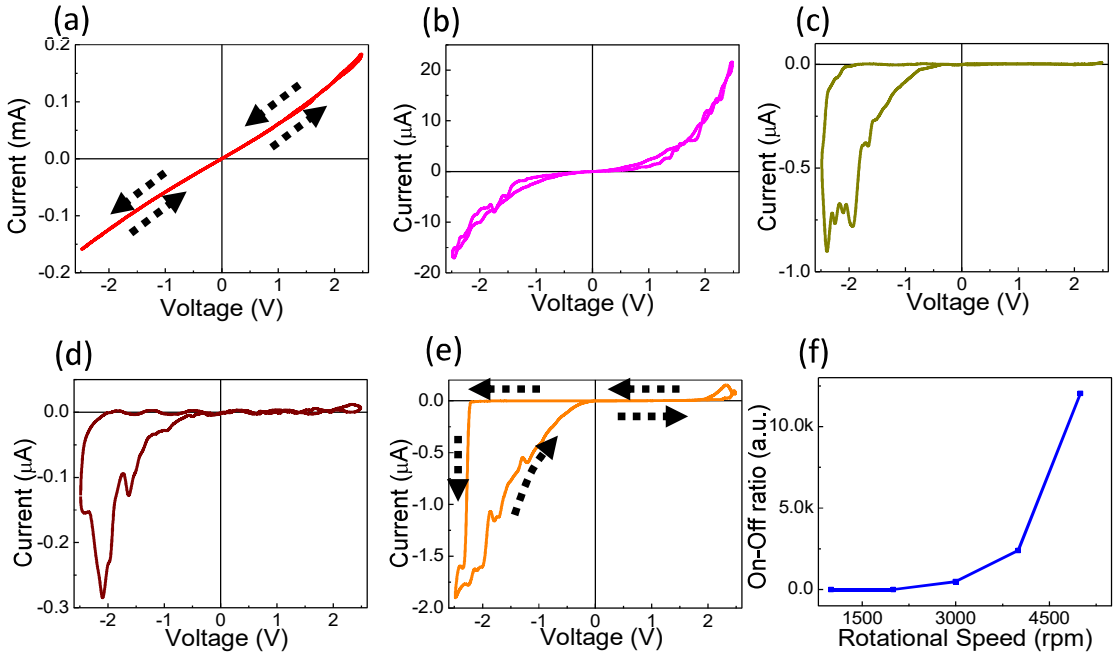

Figure 4.5: (a) – (e) I-V characteristics for the devices fabricated at 1000 – 5000 rpm with an increase of 1000 rpm. The arrows in (a) and (e) show the direction of voltage scan. (f) Variation of ON-OFF ratio with RPM of rotational speeds at which the devices were spin coated.

4.3.4 Switching Mechanism

To understand the switching mechanism the surface morphology of each of the devices must be recalled one by one. Starting with the lowest rotational speed (1000 rpm) device, it was observed that big pits and valleys were a dominant feature on the surface. These big holes allow direct contact of the top and the bottom electrodes. The I-V characteristics for this device agree with this conjecture of direct contact as current and voltage have a linear relationship in both positive and negative bias directions. This sort of ohmic behavior is observed with conductors only. The formation of metal filament has been verified in the earlier study by IR imaging of the device while scanning the I-V curves [Vyas *et al.*, 2016]. This situation is shown in figure 4.6(a) depicting the proposed mechanism for conduction in the device. The conduction mechanism for 2000 rpm-based device, is shown in figure 4.6(b). Since the holes present in this device are comparatively smaller than the previous case, the formation of a direct path becomes less probable which is evident from its I-V curve, which is nonlinear, and the order of current is also much less than that of 1000 rpm-based device. A lack of switching in the device shows that there is a permanent filamentary path between the top and bottom electrodes. However, it is comparatively narrower than the previous case which causes a drop in the conductance.

The AFM image of the devices fabricated at 3000 rpm, shows that the surface has many small and large structures which are fairly close to each other. The cracks between the structures allow the aluminum to fill in them to an extent. However, to completely fill these cracks, a suitable voltage bias is required. The reason for this is the cracks have become so narrow that the complete filamentary path is not formed without the help of external bias voltage. At a particular bias in the negative direction, the migration of Al ions from the top electrode to bottom electrode starts. As the voltage increases, this migration also increases, until there is a direct contact between the top and bottom electrodes. This is the point where the conductance switches to a high value. This switching into the high conductance state is called *setting* of the device. The device stays in this high conductance state until the voltage traces back to the positive bias and the filament breaks, which is called the *resetting* of the device. In this case, the ON-OFF ratio of the device is not too

high, as the off-state current is rather high. The reason for slightly higher off-state current is presence of partially conducting paths between the top and bottom electrodes. The switching mechanism in 3000 rpm device is shown in figure 4.6(c).

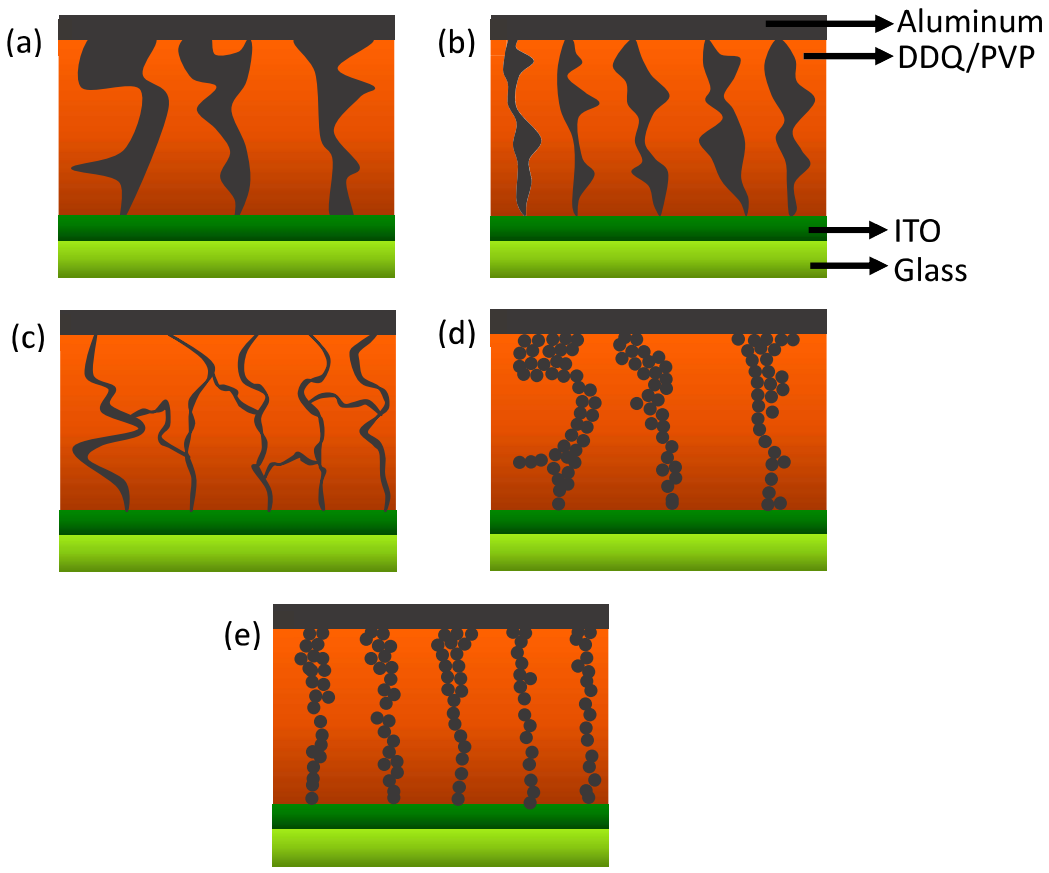

Figure 4.6: (a)-(e) Schematic of proposed model for the switching mechanism of the devices prepared with the spin coating method at the speeds ranging from 1000-5000 rpm with an increase of 1000 rpm.

At higher speeds of deposition (4000 rpm), the surface of the active layer is covered with fairly uniform small structures. The cracks between the structures are not as clearly visible as that of the previous device, hence the formation of a path becomes more difficult than it was in the previous case, resulting in a low off-state current and a higher ON-OFF ratio. Figure 4.6(d) shows the mechanism through which the switching takes place in the 4000 rpm-based devices. For the devices fabricated with the highest speed (5000 rpm), the AFM image of the surface clearly shows the presence of a few small pinholes. These pinholes allow aluminum ions to migrate through them under a suitable bias voltage. The diameter of these pinholes is very small and the number of pinholes is also less, hence the off-state current is very low, which makes the ON-OFF ratio very high. Furthermore, the decreased path length of the filament causes the conductance in the ON state to be a bit higher which makes the ON-OFF ratio significantly.

The validation of filament formation conjecture can also be given by the EDX data. The percentage of elemental aluminum in the organic layer is found to be decreasing with an increase in the rotational speed. The reason behind this decrease in the aluminum concentration is the decreasing size of holes, formation of thin cracks and small pinholes. With the decrease in the size of holes, the percolating aluminum in the holes also decreases.

4.3.5 Influence of Surface Morphology on I-V characteristics

The exponential increase in the ON-OFF ratio of the memory devices prepared with the DDQ-PVP blend with respect to the rotational speed of the spin coating process is dependent on the surface morphology. The morphology of the films changed distinctively with the increasing rotational speeds at the time of deposition. In thicker films, deposited at lower speeds, the holes are bigger. The thickness of the film is inversely proportional to the rotational speed during the spin coating process [Zhang *et al.*, 2013]. Formation of the domain is prevalent in thicker films because of the phase segregation between the two components in the film. The phase segregation indicates that film is not at the thermal equilibrium. The reason behind this is that the thicker films take a longer time to dry, which allows the domain formation during the spin coating [Walheim *et al.*, 1997; Zhang *et al.*, 2013]. At a higher speed of deposition, there is very less time available for segregation of the phase during the drying up process. Therefore, there is a lack of small or big structure at higher speeds and pinholes appear on the surface.

4.3.6 RAM and ROM Applications of the Memory Devices

The device tested at the highest speed i.e. 5000 rpm was tested for RAM and ROM applications. For a memory to be useful as RAM, the repeatability and reliability test (endurance test) is the criterion. For a switching device to be useful in the ROM applications, long retention times are required in order to prevent any logical state (0 or 1) to dwindle. To study the RAM properties of the device, a cycle of write-read-erase-read pulses of − 4, − 1.5, 4, − 1.5 V for 5, 10, 5, and 10 s, respectively, was applied to the devices for more than 1000 s, and the device was found to respond to the read voltages with a consistency.

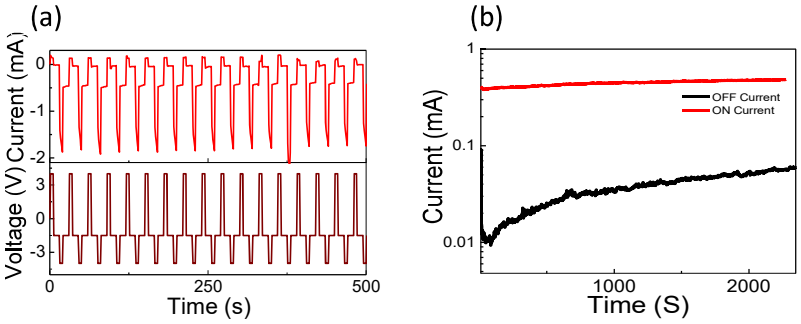

Figure 4.7: (a) The write–read–erase–read voltage pulse cycle with V_{write} = −4 V, V_{erase} = 4 V and V_{read} = − 1.5 V are applied for 5, 5, and 10 s, respectively. (b) Retention time study with V_{read} = − 1.5 V, and V_{write} and V_{erase} being − 4 and 4 V applied for 5 s, respectively. The train of current at − 1.5 V followed by write and erase voltage pulses are called as on and off state current and are measured for more than 2000 s

The ROM feature of the device was studied by subjecting the device to write or erase voltage pulses of -4V or 4V for a short time followed by a read pulse of -1.5V for a long time to test whether or not the memory device retains the previous logical state for a long time. The device with 5000 rpm showed good stability in both high and low conductance state for 2 x 10^3s. Figure 4.7 shows the endurance and retention characteristics of the device deposited at 5000 rpm. A higher value of Erase and Write voltages was chosen because the read states after that voltage were more stable.

4.4 CONCLUSION

In conclusion, the small molecule – polymer blend memory devices were fabricated using the spin coating method at various rotational speeds in the range of 1000-5000 rpm. The thickness of the devices decreased with the increase in rotational speed. Examination of surface morphology of the films revealed a distinct trend in the topography. At lower rotational speeds, the surface

had many big holes and domains in it, whereas the films fabricated at a high rotational speed (5000 rpm) had small pinholes in them. Phase segregation of the two components in the mixture, which depends on the speed of rotation, is the reason for the formation of the pits and valleys at lower speeds and pinholes at higher speeds. At higher speeds, time available for the phase segregation is less than at the lower speeds. Furthermore, this trend in surface morphology leads to an exponential increase in the on-off ratio of the memory devices and provides us with a means to tune the ON-OFF ratio of the devices by controlling the rotational speeds during the spin coating process.